arXiv:2001.04209v1 [cond-mat.mes-hall] 13 Jan 2020

Non-Hermitian Avalanche Effect – Non-Perturbative Effect Induced by Local Non-Hermitian Perturbation on a Z_2 Topological Order

Cui-Xian Guo,[1] Xiao-Ran Wang,[1] and Su-Peng Kou[1,*]

[1] *Center for Advanced Quantum Studies, Department of Physics, Beijing Normal University, Beijing 100875, China*

In this paper, based on a non-Hermitian toric-code model, we surprisingly find that the degeneracy of ground states can be changed by a local non-Hermitian perturbation (even in thermodynamic limit). We call it non-Hermitian avalanche effect. As the physics consequences of the non-Hermitian avalanche effect, a correspondence between bulk quasi-particles and topologically protected degenerate ground states for Z_2 topological order is borken down. In addition, the PT symmetry breaking transition of the topologically degenerate ground states subspace can be observed by fidelity susceptibility.

I. INTRODUCTION

Recently, there has been a lot of activities in the research on non-Hermitian topological systems[1–38], including non-Hermitian topological insulators, non-Hermitian topological superconductors, and non-Hermitian topological semi-metals. After considering the non-Hermitian extensions of the usual topological band systems, quantum exotic effects are uncovered, such as the fractional topological invariant and defective edge states[6, 17], non-Hermitian skin effect[14, 21, 24, 35, 37], and the breakdown of bulk-boundary correspondence[11, 14–16, 30–32, 34, 37]. In addition to the research on non-Hermitian topological band systems, the non-Hermitian extensions of intrinsic topological orders that are many-body topological systems with long range entanglement are studied[39, 40]. In Ref.[39], the non-Hermitian strings and the breakdown of the correspondence between bulk quasi-particles and topologically protected degenerate ground states are discovered. In Ref.[40], a continuous quantum phase transition without gap closing was explored that occurs in non-Hermitian topological orders together with the breakdown of the Lieb-Robinson bound.

Therefore, one must give it careful reconsideration on the non-Hermitian extensions of topological stability for intrinsic topological orders. It was well known that for the topological ordered states, due to the existence of energy gap, the ground states are robust. The degeneracy of the ground states depends on the topology of the system and is also robust against any small and local perturbations. Topological phase transition between topological ordered states and trivial states may occur when the perturbations become large enough and are beyond certain thresholds.

In this paper, we will study topological stability for intrinsic topological orders under non-Hermitian perturbations by taking the non-Hermitian toric-code model as an example. The effect of non-Hermitian avalanche for a designed toric-code model is uncovered: for the designed toric-code model with special external fields, a tiny non-Hermitian perturbation (local imaginary state selective dissipation) leads to anomalous topological degeneracy and the breakdown of bulk-degeneracy correspondence (a correspondence between bulk quasi-particles and topologically protected degenerate ground states).

II. TOPOLOGICAL STABILITY OF (HERMITIAN) Z_2 TOPOLOGICAL ORDER

Firstly, we show the topological stability of (Hermitian) Z_2 topological order.

For a Z_2 topological order, there are four types of topological sectors (ground state and three types of quasi-particles), 1 (vacuum), e (e-particle or Z_2 charge), m (m-particle or Z_2 vortex), f (fermion). e-particle and m-particle are all bosons with mutual π statistics between them. The fermion can be regarded as a bound state of an e-particle and an m-particle. All these quasi-particles have finite energy gaps Δ^I, (I = e, m, f). The four kinds of topological sectors is denoted by $\mathcal{N} = 4$ where $\mathcal{N}$ denotes the number of topological sector of quasi-particles. When we consider the perturbations on the systems, the energy gaps Δ^I may change slightly, $\Delta^I \to (\Delta^I)' = \Delta^I + \delta\Delta^I$ ($\delta\Delta^I \ll \Delta^I$) and cannot be closed. That indicate all perturbations are irrelevant.

When we consider the system on a torus, the ground states have topological degeneracy. Each degenerate ground state $|0\rangle_I$ corresponds to the one by adding a virtual quasi-particle. We can use the basis of sectors of (virtual) quasi-particles to characterize the ground states, i.e.,

$$(|0\rangle, |e\rangle, |m\rangle, |f\rangle)\,. \tag{1}$$

This is named *bulk-degeneracy correspondence* (BDC). We denote the BDC by

$$\mathcal{N}(=4) = \mathcal{D}, \tag{2}$$

where $\mathcal{D}$ denotes the number of ground state degeneracy. For a system with infinite size, the four ground

*Corresponding author; Electronic address: spkou@bnu.edu.cn

states $(|0\rangle, |e\rangle, |m\rangle, |f\rangle)$ become degenerate with exact zero energy splitting. When one considers the perturbations on the systems, the degeneracy of the four ground states doesn't change. In Ref.[41], it is pointed out that the topological-order classes are stable against any small stochastic local transformations and there exists a phenomenon of emergence of unitarity.

We use the Kitaev's toric-code model as an example to illustrate the topological stability of (Hermitian) Z_2 topological order. The toric-code model is an exactly solvable spin model, of which the Hamiltonian is

$$\hat{H}_{TC} = -g(\sum_s A_s + \sum_p B_p), \tag{3}$$

where $A_s = \prod_{i\in s}\sigma_i^x$ and $B_p = \prod_{i\in p}\sigma_i^z$, the subscripts s and p represent the vertices and plaquettes of a square lattice, respectively. In this paper, we set $g \equiv 1$. For the toric-code model, the ground states are defined as $A_s|\psi_g\rangle = |\psi_g\rangle$, $B_p|\psi_g\rangle = |\psi_g\rangle$ for all A_s and B_p. Furthermore, the elementary excitations are defined as $A_s = -1$ and $B_p = -1$.

The quantum states of Z_2 topological order are characterized by different configurations of strings, $\hat{W}(C) = \prod_{i\in C}\sigma_i^{\alpha_i}$ where $\sigma_i^{\alpha_i}$ is α_i-type Pauli matrix on site i and $\prod_{i\in C}$ is over all the sites on the string along a loop C, i.e., $|\Phi\rangle = \sum_C a_C\hat{W}(C)|0\rangle$ where $|0\rangle$ denotes the spin polarized states with all spin down $(|\downarrow\downarrow, ..., \downarrow\rangle)$, $\hat{W}(C)$ denotes the possible string operators, and a_C is weight of the string operator. The different configurations of open strings correspond to different excited states of different quasi-particles. For e-particle/m-particle, the string connects the nearest neighboring odd (even) sub-plaquettes

$$\hat{W}_{c/v}(C) = \prod_{i\in C}\sigma_i^{s_{c/v}}, \tag{4}$$

where the product $\prod_{i\in C}$ is over all the sites on the string along a loop C connecting odd-plaquettes (or even-plaquettes), $s_c = z$ and $s_v = x$. The string for f-particles is defined as

$$\hat{W}_f(C) = \hat{W}_v(C)\hat{W}_c(C) = \prod_{i\in C}\sigma_i^{s_f}, \tag{5}$$

where $s_f = y$. We point out that the local perturbations on the Z_2 topological order just locally, and slightly deform the string configurations but can never change the degeneracy of ground states.

In addition, for the toric-code model, the dissipation effect had been studied in Ref[42]. The results show that small dissipations cannot change the ground states. As a result, the degenerate ground states make up a protected code subspace and can be regarded as topological qubits to do possible topological quantum computation [44].

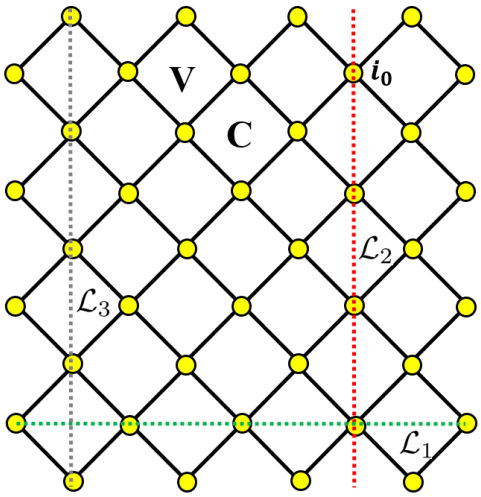


FIG. 1: (Color online) The schematic diagram of the designed toric-code model. The external fields are applied only on three paths.

III. DESIGNED TORIC-CODE MODEL AND ITS DEGENERATE GROUND STATES

In this section, we introduce the designed toric-code model, of which the Hamiltonian is expressed as

$$\hat{H}'_{TC} = \hat{H}_{TC} + \hat{H}', \tag{6}$$

where

$$\hat{H}' = h_x\sum_{i\in\mathcal{L}_1}\sigma_i^x + h_z\sum_{i\in\mathcal{L}_2}\sigma_i^z + h'_x\sum_{i\in\mathcal{L}_3}\sigma_i^x. \tag{7}$$

Here, h_x, h_z and h'_x are real parameters, and h'_x is a small real parameter. The dominating external fields are applied only on two crossing lines ($\mathcal{L}_1$ and $\mathcal{L}_2$). In addition, the auxiliary external fields are applied on $\mathcal{L}_3$. See the illustration in Fig.1.

Under the perturbation $\hat{H}' = h_x\sum_{i\in\mathcal{L}_1}\sigma_i^x + h_z\sum_{i\in\mathcal{L}_2}\sigma_i^z + h'_x\sum_{i\in\mathcal{L}_3}\sigma_i^x$, the quasi-particles begin to hop. The terms $h_x\sum_{i\in\mathcal{L}_1}\sigma_i^x$ and $h'_x\sum_{i\in\mathcal{L}_3}\sigma_i^x$ drives the m-particle without affecting fermion and e-particle along $\mathcal{L}_1$ string and $\mathcal{L}_3$ string, respectively. The term $h_z\sum_{i\in\mathcal{L}_2}\sigma_i^z$ drives the e-particle without affecting fermion and m-particle along $\mathcal{L}_2$ string.

The ground state for $\hat{H}_{TC}$ is a Z_2 topological order[44–46]. The ground states have topological degeneracy, i.e., different topologically degenerate ground states are classified by different topological closed operation strings $\hat{W}_a(C^{\text{close,topo}})$. The operator $\hat{W}_a(C^{\text{close,topo}})$ takes on binary values 0, 1 and denotes whether the loops $C^{\text{close,topo}}$ belong to the even or odd winding number sectors along the x/y-direction. So, we can use the basis of even-odd parity of the winding number of electric field lines around the torus $|m_{ab}\rangle$, $(\ |0,0\rangle\ \ |0,1\rangle\ \ |1,0\rangle\ \ |1,1\rangle\ )$. For a $Z2$ topological order

with 4 degenerate ground states, there exist the following equations that illustrate the relationship between the basis of even-odd parity of the winding number of electric field lines around the torus $|m_{ab}\rangle$ $(a,b=0,1)$ and the basis of topological sectors labeled by different quasiparticles,

$$\begin{pmatrix} |0\rangle \\ |e\rangle \\ |m\rangle \\ |f\rangle \end{pmatrix} = U \begin{pmatrix} |0,0\rangle \\ |0,1\rangle \\ |1,0\rangle \\ |1,1\rangle \end{pmatrix} U^{-1}$$

where

$$U = \frac{1}{\sqrt{2}} \begin{pmatrix} 1 & 1 & 0 & 0 \\ 1 & -1 & 0 & 0 \\ 0 & 0 & 1 & 1 \\ 0 & 0 & 1 & -1 \end{pmatrix}.$$

As a result, the bulk-degeneracy correspondence is valid, i.e.,

$$\mathcal{N}(=4) = \mathcal{D}. \tag{8}$$

We use a four-level system to describe the topologically degenerate ground states[46]. After considering $\hat{H}'$, three quantum tunneling processes occur: (1) virtual Z_2-vortex propagating along $\mathcal{L}_1$ ($\hat{e}_x$ direction); (2) virtual Z_2-charge propagating along $\mathcal{L}_2$ ($\hat{e}_y$ direction); (3) virtual Z_2-vortex propagating along $\mathcal{L}_3$ ($\hat{e}_y$ direction) around the torus. With the help of the high-order purterbative theory, the four-level quantum system of the four nearly degenerate ground states on a $2*L_x*L_y$ lattice (with $2*L_x*L_y$ spins) is obtained

$$\hat{\mathcal{H}}_{\text{eff}}^{L_x*L_y} = \Delta(\tau_1^x \otimes 1) + \varepsilon(\tau_1^z \otimes \tau_2^x) + \kappa(1 \otimes \tau_2^x), \tag{9}$$

where $\Delta = (\alpha h_x)^{L_x}$, $\varepsilon = (\alpha h_z)^{L_y}$ and $\kappa = (\alpha h_x')^{L_y}$ (α is real parameter). The eigenvalues of $\hat{\mathcal{H}}_{\text{eff}}^{L_x*L_y}$ can be obtained as $\pm\kappa \pm \sqrt{\Delta^2+\varepsilon^2}$.

IV. TOPOLOGICAL POISONING EFFECT OF THE NON-HERMITIAN TOPOLOGICAL ORDER

We then take the toric-code model as an example to illustrate the string poisoning effect by considering the non-Hermitian local perturbations. Here, the non-Hermitian toric-code model is defined by adding non-Hermitian external fields,

$$\hat{H}''_{NTC} = \hat{H}_{TC} + \hat{H}'', \tag{10}$$

where

$$\hat{H}'' = \sum_i \mathbf{h}_i \cdot \sigma_i = \sum_i h_i^x \sigma_i^x + \sum_i h_i^y \sigma_i^y + \sum_i h_i^z \sigma_i^z. \tag{11}$$

Now, we introduce $\mathbf{h}_i \neq \mathbf{h}_i^*$ for ith-spin, therefore the Hamiltonian satisfies $\hat{H}''_{NTC} \neq \hat{H}''^*_{NTC}$.

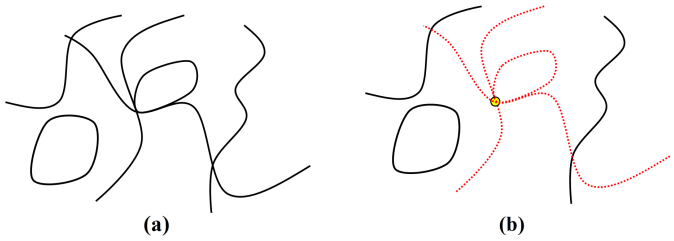


FIG. 2: (Color online) The schematic diagram of topological poisoning effect: (a) The Hermitian (dynamic) strings for the Hermitian Z2 topological order; (b) Arbitrary dynamic strings passing through site i_0 (long or short) become non-Hermitian. This is the physics consequence of topological poisoning effect by adding local non-Hermitian perturbation on site i_0, i.e., $D_a(C_N \rightsquigarrow i_0)$.

To characterize the quantum properties of the non-Hermitian Z_2 topological order, the (non-Hermitian) dynamic strings were defined as[39]

$$D_a(C_N) = \prod_{i\in C} \frac{\hat{t}_i^a}{|\hat{t}_i^a|} = \prod_{i\in C} h_i^a \sigma_i^a,$$

where $h_i^a\sigma_i^a$ acts at step i for a-type excitation and the indices $a = v,\ c,\ f$ correspond to three types of quasiparticles. For the case of $D_a(C_N) \neq D_a^\dagger(C_N)$, a dynamical string becomes non-Hermitian. To study its non-Hermitian property, we had introduced the biorthogonal set for the quantum string states of Z_2 topological order.

In this paper, we consider the non-Hermitian model with local non-Hermitian external field on single lattice site i_0, i.e.,

$$\mathbf{h}_{i_0} \neq \mathbf{h}_{i_0}^*,\ \mathbf{h}_{i\neq i_0} = \mathbf{h}_{i\neq i_0}^*. \tag{12}$$

Now, arbitrary dynamic strings passing through site i_0 (long or short) becomes non-Hermitian,

$$D_a(C_N \rightsquigarrow i_0) \neq D_a^\dagger(C_N \rightsquigarrow i_0), \tag{13}$$

where $C_N \rightsquigarrow i_0$ means the pathes crossing site i_0. We call it *topological poisoning effect* under local non-Hermitian perturabtions. Due to the topological poisoning effect, a local non-Hermitian perturabtion (for example, $\mathbf{h}_{i_0}$ at non-Hermitian external field at site i_0) may causes highly non-local influence. See the illustration in Fig.2. The red dashed strings are all non-Hermitian dynamic strings poisoned by the local non-Hermitian perturbations at site i_0.

V. NON-HERMITIAN AVALANCHE EFFECT

A. Local non-Hermitian perturbation

Now, we consider a particular local non-Hermitian perturbation on the designed toric-code model,

$$\hat{H}_{NTC} = \hat{H}'_{TC} + \hat{H}'' = \hat{H}_{TC} + \hat{H}' + \hat{H}'', \tag{14}$$

where

$$\hat{H}'' = (\lambda_{\rm Re} + i\lambda_{\rm Im})\sigma^z_{i_0}. \quad (15)$$

It is obvious that $\hat{H}_{NTC}$ doesn't have Parity-time symmetry. However, an important changes is topological poisoning effect under local non-Hermitian perturabtions, $D_a(C_N \rightsquigarrow i_0)$.

When considering above extra non-Hermitian term, the effective Hamiltonian of the degenerate ground states $\hat{\mathcal{H}}^{L_x*L_y}_{\rm eff}$ on designed toric-code model may change:

1. When the site i_0 is on vertical dynamic string $\mathcal{L}_2$, $\hat{\mathcal{H}}^{L_x*L_y}_{\rm eff}$ becomes

$$\hat{\mathcal{H}}^{L_x*L_y}_{\rm eff} = \Delta(\tau^x_1 \otimes 1) + \varepsilon'(\tau^z_1 \otimes \tau^x_2) + \kappa(1 \otimes \tau^x_2), \quad (16)$$

   where $\Delta = (\alpha h_x)^{L_x}$, $\varepsilon' = \alpha^{L_y}(h_z)^{L_y-1}(h_z + \lambda_{\rm Re} + i\lambda_{\rm Im})$ and $\kappa = (\alpha h'_x)^{L_y}$. The eigenvalues of $\hat{\mathcal{H}}^{L_x*L_y}_{\rm eff}$ can be obtained as $\pm\kappa \pm \sqrt{\Delta^2 + (\varepsilon')^2}$;

2. When the site i_0 is on transverse dynamic string $\mathcal{L}_1$, $\hat{\mathcal{H}}^{L_x*L_y}_{\rm eff}$ becomes

$$\hat{\mathcal{H}}^{L_x*L_y}_{\rm eff} = \Delta'(\tau^x_1 \otimes 1) + \varepsilon(\tau^z_1 \otimes \tau^x_2) + \kappa(1 \otimes \tau^x_2), \quad (17)$$

   where $\Delta' = \alpha^{L_x}(h_x)^{L_x-1}(h_x + \lambda_{\rm Re} + i\lambda_{\rm Im})$, $\varepsilon = (\alpha h_z)^{L_y}$ and $\kappa = (\alpha h'_x)^{L_y}$. The eigenvalues of $\hat{\mathcal{H}}^{L_x*L_y}_{\rm eff}$ can be obtained as $\pm\kappa \pm \sqrt{(\Delta')^2 + \varepsilon^2}$;

3. When the site i_0 is on crossing between $\mathcal{L}_1$ and $\mathcal{L}_2$, $\hat{\mathcal{H}}^{L_x*L_y}_{\rm eff}$ becomes

$$\hat{\mathcal{H}}^{L_x*L_y}_{\rm eff} = \Delta'(\tau^x_1 \otimes 1) + \varepsilon'(\tau^z_1 \otimes \tau^x_2) + \kappa(1 \otimes \tau^x_2), \quad (18)$$

   where $\Delta' = \alpha^{L_x}(h_x)^{L_x-1}(h_x + \lambda_{\rm Re} + i\lambda_{\rm Im})$, $\varepsilon' = \alpha^{L_y}(h_z)^{L_y-1}(h_z + \lambda_{\rm Re} + i\lambda_{\rm Im})$ and $\kappa = (\alpha h'_x)^{L_y}$. The eigenvalues of $\hat{\mathcal{H}}^{L_x*L_y}_{\rm eff}$ can be obtained as $\pm\kappa\pm \sqrt{(\Delta')^2 + (\varepsilon')^2}$;

4. When the site i_0 is not on dynamic strings ($\mathcal{L}_1$, $\mathcal{L}_2$ and $\mathcal{L}_3$), $\hat{\mathcal{H}}^{L_x*L_y}_{\rm eff}$ doesn't change. The eigenvalues of $\hat{\mathcal{H}}^{L_x*L_y}_{\rm eff}$ can be obtained as $\pm\kappa \pm \sqrt{\Delta^2 + \varepsilon^2}$.

In this paper, we focus on the case 1 and $\hat{H}'' = -h_z + ih_z\sigma^x_{i_0}$. Therefore, The eigenvalues of $\hat{\mathcal{H}}^{L_x*L_y}_{\rm eff}$ can be obtained as $E_\pm = \pm\kappa \pm \sqrt{\Delta^2 - \varepsilon^2}$.

B. Spontaneous PT-symmetry breaking

When the site i_0 is on vertical dynamic string $\mathcal{L}_2$ and $\hat{H}'' = -h_z + ih_z\sigma^x_{i_0}$, we have $\varepsilon' = i\varepsilon$. Then $\hat{\mathcal{H}}^{L_x*L_y}_{\rm eff}$ becomes

$$\hat{\mathcal{H}}^{L_x*L_y}_{\rm eff} = \Delta(\tau^x_1 \otimes 1) + i\varepsilon(\tau^z_1 \otimes \tau^x_2) + \kappa(1 \otimes \tau^x_2), \quad (19)$$

where $\Delta = (\alpha h_x)^{L_x}$, $\varepsilon = (\alpha h_z)^{L_y}$ and $\kappa = (\alpha h'_x)^{L_y}$. The effective Hamiltonian $\hat{\mathcal{H}}^{L_x*L_y}_{\rm eff}$ has PT symmetry. The eigenvalues of $\hat{\mathcal{H}}^{L_x*L_y}_{\rm eff}$ can be obtained as

$$\begin{aligned} &E_1 = -\kappa - \sqrt{\Delta^2 - \varepsilon^2}, \quad E_2 = -\kappa + \sqrt{\Delta^2 - \varepsilon^2}, \\ &E_3 = \kappa - \sqrt{\Delta^2 - \varepsilon^2}, \quad E_4 = \kappa + \sqrt{\Delta^2 - \varepsilon^2}. \end{aligned} \quad (20)$$

When the site i_0 is on vertical dynamic string, for the case of $|\Delta| \geq |\varepsilon|$, the system belongs to a phase with $\mathcal{PT}$ symmetry, of which E are real and the eigenvectors are eigenstates of the symmetry operator, i.e., $\mathcal{PT}|\varphi_i\rangle = |\varphi_i\rangle$. For the case of $|\Delta| < |\varepsilon|$, E are complex, and $\mathcal{PT}|\varphi_i\rangle \neq |\varphi_i\rangle$. A $\mathcal{PT}$-symmetry-breaking transition occurs at the exceptional points $|\Delta| = |\varepsilon|$, which leads to the following relation $h_x = h_z$ when $L_x = L_y$. It is clear that $|\psi_1\rangle$ and $|\psi_2\rangle$ compose a pair of $\mathcal{PT}$-symmetry, and $|\psi_3\rangle$ and $|\psi_4\rangle$ compose another pair of $\mathcal{PT}$-symmetry.

The eigenstates $|\varphi_i\rangle$ of $\hat{\mathcal{H}}^{L_x*L_y}_{\rm eff}$ can be written as

$$|\psi_1\rangle = \frac{1}{\rm N_1}\begin{pmatrix} \frac{i\varepsilon+\sqrt{\Delta^2-\varepsilon^2}}{\Delta} \\ \frac{-\Delta^2+(\varepsilon-i\sqrt{\Delta^2-\varepsilon^2})(\varepsilon-i\kappa)}{\Delta(\sqrt{\Delta^2-\varepsilon^2}+\kappa)} \\ -1 \\ 1 \end{pmatrix},$$

$$|\psi_2\rangle = \frac{1}{\rm N_2}\begin{pmatrix} \frac{i\varepsilon-\sqrt{\Delta^2-\varepsilon^2}}{\Delta} \\ \frac{\Delta^2+(-\varepsilon-i\sqrt{\Delta^2-\varepsilon^2})(\varepsilon-i\kappa)}{\Delta(\sqrt{\Delta^2-\varepsilon^2}-\kappa)} \\ -1 \\ 1 \end{pmatrix},$$

$$|\psi_3\rangle = \frac{1}{\rm N_3}\begin{pmatrix} \frac{i\varepsilon-\sqrt{\Delta^2-\varepsilon^2}}{\Delta} \\ \frac{-\Delta^2+(\varepsilon+i\sqrt{\Delta^2-\varepsilon^2})(\varepsilon-i\kappa)}{\Delta(\sqrt{\Delta^2-\varepsilon^2}-\kappa)} \\ 1 \\ 1 \end{pmatrix},$$

and

$$|\psi_4\rangle = \frac{1}{\rm N_4}\begin{pmatrix} \frac{i\varepsilon+\sqrt{\Delta^2-\varepsilon^2}}{\Delta} \\ \frac{\Delta^2+(-\varepsilon+i\sqrt{\Delta^2-\varepsilon^2})(\varepsilon-i\kappa)}{\Delta(\sqrt{\Delta^2-\varepsilon^2}+\kappa)} \\ 1 \\ 1 \end{pmatrix}, \quad (21)$$

where $\rm N_i$ $(i = 1, 2, 3, 4)$ are normalization constant. In the region of $\mathcal{PT}$-unbroken phase ($|\Delta| \geq |\varepsilon|$), the normalization constant are obtained as $\mathcal{N}_1 = \mathcal{N}_2 = \mathcal{N}_3 = \mathcal{N}_4 = 2$. And in the region of $\mathcal{PT}$-broken phase ($|\Delta| < |\varepsilon|$), the normalization constant are obtained as $\mathcal{N}_1 = \mathcal{N}_4 = \frac{2\sqrt{\varepsilon^2+\varepsilon\sqrt{\varepsilon^2-\Delta^2}}}{\Delta}$, $\mathcal{N}_2 = \mathcal{N}_3 = \frac{2\sqrt{\varepsilon^2-\varepsilon\sqrt{\varepsilon^2-\Delta^2}}}{\Delta}$.

From the result, one can see there exist exceptional points (EPs) at $|\Delta| = |\varepsilon|$. In the limit of $\Delta \to 0$, $\varepsilon \to 0$ according to the condition of quantum phase transition ($|\Delta| = |\varepsilon|$), an arbitrary small local perturbation (a local complex external field) causes the quantum phase transition for the ground states. We call it *non-Hermitian avalanche effect*. In the followings, we show the physics consequences of the non-Hermitian avalanche effect - breakdowns of bulk-degeneracy correspondence for Z2 topological order.

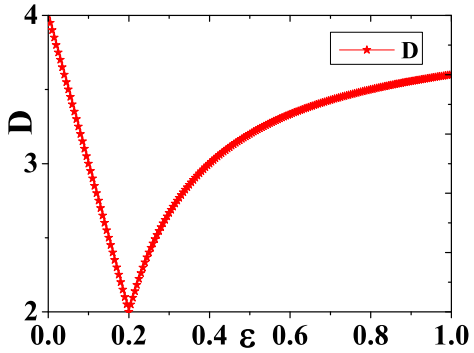


FIG. 3: (Color online) The non-Hermitian degeneracy that is away from 4. At exceptional point, it is 2.

C. Breakdowns of bulk-degeneracy correspondence for Z2 topological order

To characterize the non-Hermitian avalanche effect, we define the (non-Hermitian) degeneracy $\mathcal{D}$ under local non-Hermitian perturbation.

Firstly, we define the overlap of any two of these four nearly degenerate eigenstates as follows,

$$\begin{aligned} &O_{12} = |\langle\psi_2|\psi_1\rangle|,\ O_{13} = |\langle\psi_3|\psi_1\rangle|,\ O_{14} = |\langle\psi_4|\psi_1\rangle|,\\ &O_{23} = |\langle\psi_3|\psi_2\rangle|,\ O_{24} = |\langle\psi_4|\psi_2\rangle|,\ O_{34} = |\langle\psi_4|\psi_3\rangle|. \end{aligned} \tag{22}$$

By inserting Eq.(21) into Eq.(22) , we obtain the overlap as

$$\begin{aligned} &O_{12} = |\frac{\varepsilon}{\Delta}|,\ O_{34} = |\frac{\varepsilon}{\Delta}|,\\ &O_{13} = 0,\ O_{23} = 0,\ O_{24} = 0,\ O_{14} = 0, \end{aligned} \tag{23}$$

in the region of $\mathcal{PT}$-unbroken phase ($|\Delta| \geq |\varepsilon|$), and

$$\begin{aligned} &O_{12} = |\frac{\Delta}{\varepsilon}|,\ O_{34} = |\frac{\Delta}{\varepsilon}|,\\ &O_{13} = 0,\ O_{23} = 0,\ O_{24} = 0,\ O_{14} = 0, \end{aligned} \tag{24}$$

in the region of $\mathcal{PT}$-broken phase ($|\Delta| < |\varepsilon|$).

Then, we define the degeneracy of ground states in this case as $\mathcal{D} = 4 - O_{12} - O_{34}$. According to the results in Fig.3, the degeneracy becomes change under the non-Hermitian strength. As a result, the bulk-degeneracy correspondence is broken, i.e.,

$$\mathcal{N}(=4) \neq \mathcal{D}(=4 - O_{12} - O_{34}). \tag{25}$$

D. Fidelity susceptibility of ground state

To confirm the existence of the quantum phase transition from non-Hermitian avalanche effect, we calculate the fidelity susceptibility of ground state.

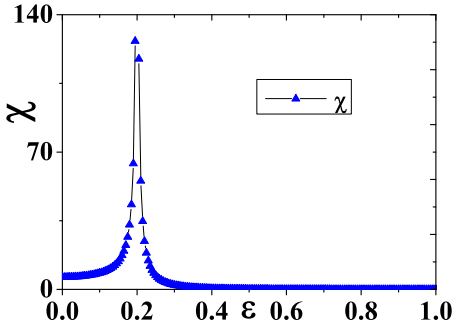


FIG. 4: (Color online) The fidelity susceptibility of ground states in terms of ε.

Fidelity susceptibility of ground state can be used to characterize the occurrence of the quantum phase transitions. In this section, we study fidelity susceptibility of a given ground state $|\psi_i\rangle (i = 1, 2, 3, 4)$ in non-Hermitian toric-code model. The fidelity of ground state in terms of ε can be defined as

$$F(\varepsilon, \delta) = |\langle\psi_i(\varepsilon)|\psi_i(\varepsilon + \delta)\rangle|. \tag{26}$$

The fidelity susceptibility of ground state in terms of ε can be defined as

$$\chi(\varepsilon, \delta) = \lim_{(\delta\to 0)} \frac{-2\ln F}{\delta^2}. \tag{27}$$

The behavior of $|\psi_i\rangle$ of the effective model $\hat{\mathcal{H}}_{\text{eff}}^{L_x * L_y} = \Delta(\tau_1^x \otimes 1) + \varepsilon(\tau_1^z \otimes \tau_2^x)$ $(\kappa \to 0)$ is same as that of $H = \Delta\tau_1^x + \varepsilon\tau_1^z$. As a result, the fidelity and fidelity susceptibility of each ground state are obtained as

$$F(\varepsilon, \delta) = \begin{cases} 1 - \frac{\delta^2}{8(\Delta^2 - \varepsilon^2)}, & |\Delta| \geq |\varepsilon| \\ 1 - \frac{\Delta^2\delta^2}{8\varepsilon^2(\varepsilon^2 - \Delta^2)}, & |\Delta| < |\varepsilon| \end{cases}, \tag{28}$$

and

$$\chi(\varepsilon, \delta) = \begin{cases} \frac{1}{4(\Delta^2 - \varepsilon^2)}, & |\Delta| \geq |\varepsilon| \\ \frac{\Delta^2}{4\varepsilon^2(\varepsilon^2 - \Delta^2)}, & |\Delta| < |\varepsilon| \end{cases}. \tag{29}$$

In Fig.4, we plot the fidelity susceptibility of ground states in terms of ε.

E. Numerical calculations of the non-Hermitian toric-code model

To support our theoretical predictions, we do numerical calculations based on the non-Hermitian toric-code model $\hat{H}_{NTC}$ on $2 * 2 * 2$lattice and on $2 * 3 * 3$ lattice.

In Fig.5, we plot the numerical results from the exact diagonalization technique of the non-Hermitian toric code model $\hat{H}_{NTC}$ on $2 * 2 * 2$ lattice with periodic boundary conditions. Fig.5 shows the global phase diagram of $\mathcal{PT}$-symmetry-breaking transition for topologically degenerate ground states. The phase boundary

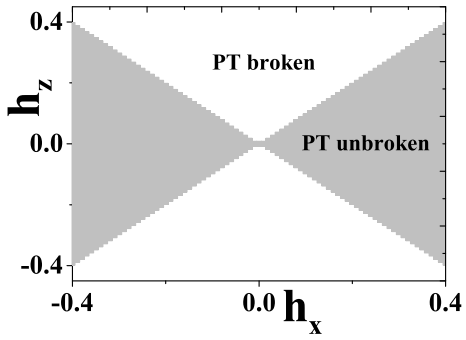


FIG. 5: (Color online) Phase diagram for spontaneous PT-symmetry breaking for the topologically degenerate ground states on $2*2*2$ lattice: in white regions, PT-symmetry is broken; in the dark regions, PT-symmetry is not broken. The phase boundaries are exceptional points.

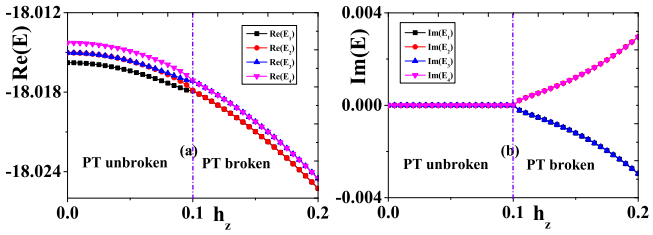


FIG. 6: (Color online) (a) The real part of energy for the four degenerate ground states for the case of $h_x = 0.1$ and $h'_x = 0.1$ via h_z based on the non-Hermitian toric-code model on $2*3*3$ lattice; (b) The imaginary of energy for the four degenerate ground states for the case of $h_x = 0.1$ and $h'_x = 0.1$ via h_z based on the non-Hermitian toric-code model on $2*3*3$ lattice.

are all exceptional points characterized by the relation $(\alpha h_x)^2 = (\alpha h_z)^2$.

In Fig.6, we plot the numerical results from the exact diagonalization technique of the non-Hermitian toric-code model $\hat{H}_{NTC}$ on $2*3*3$ lattice with periodic boundary conditions. Fig.6 shows the real part and imaginary part of energy for the four nearly degenerate ground states for the non-Hermitian toric-code model with $h_x = 0.1$ and $h'_x = 0.1$ on $2*3*3$lattice, respectively. The numerical results indicate that exceptional points occur when $h_x = h_z$, which is consistent with theoretical prediction.

In addition, we calculate the overlap of any two of these four nearly degenerate eigenstates O_{ij}defined as above. We theoretically predict that the overlaps are

$$O_{12} = O_{34} = |\frac{\varepsilon}{\Delta}| \sim \begin{cases} \frac{h_z^2}{h_x^2} & (2*2*2 \text{ lattice}) \\ \frac{h_z^3}{h_x^3} & (2*3*3 \text{ lattice}) \end{cases} \quad (30)$$
$$O_{13} = O_{23} = O_{24} = O_{14} = 0,$$

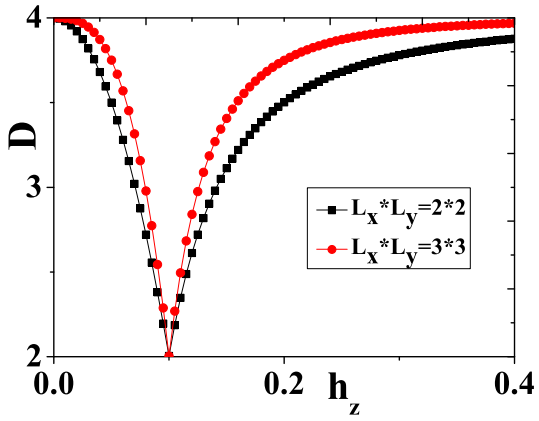


FIG. 7: (Color online) The non-Hermitian degeneracy for the ground states for the case of $h_x = 0.1$ and $h'_x = 0.1$ via h_z based on the non-Hermitian toric-code model on $2*2*2$ lattice and those on $2*3*3$ lattice.

in $\mathcal{PT}$-unbroken phase. In addition,

$$O_{12} = O_{34} = |\frac{\Delta}{\varepsilon}| \sim \begin{cases} \frac{h_x^2}{h_z^2} & (2*2*2 \text{ lattice}) \\ \frac{h_x^3}{h_z^3} & (2*3*3 \text{ lattice}) \end{cases} \quad (31)$$
$$O_{13} = O_{23} = O_{24} = O_{14} = 0,$$

in $\mathcal{PT}$-broken phase.

In Fig.7, we present the numerical results from the exact diagonalization technique of the non-Hermitian toric-code model on $2*2*2$ and $2*2*3$ lattices with periodic boundary conditions, respectively. We plot the the non-Hermitian degeneracy as a function of h_z for the case of $h_x = 0.1$ and $h'_x = 0.1$, which is consistent with the theoretical prediction. The results indicate the degeneracy of ground states may be different from 4. Now, he bulk-degeneracy correspondence is broken, i.e.,

$$\mathcal{N}(=4) \neq \mathcal{D}. \quad (32)$$

In Fig.8, we show the fidelity susceptibility of the ground state from the exact diagonalization technique of the non-Hermitian toric-code model on $2*2*2$ and $2*2*3$ lattices with periodic boundary conditions, respectively. The results show that the quantum PT phase transition occurs at EPs.

VI. CONCLUSION

In this paper, we study the non-Hermitian avalanche effect induced by a local non-Hermitian perturbation. we investigate the effective models for topological degenerate ground states of the designed non-Hermitian toric-code model by high-order degenerate perturbation theory. In particular, there exists spontaneous $\mathcal{PT}$- symmetry breaking for the topologically degenerate ground

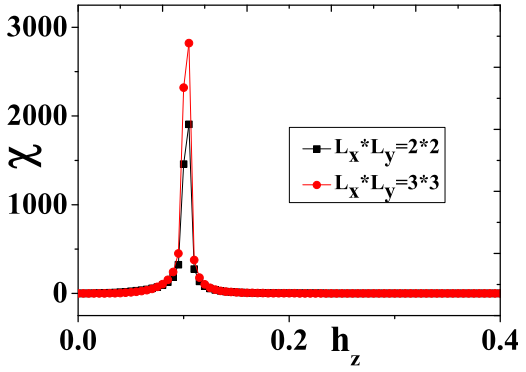


FIG. 8: (Color online) The fidelity susceptibility for the ground states for the case of $h_x = 0.1$ and $h'_x = 0.1$ via h_z based on the non-Hermitian toric-code model on $2 * 2 * 2$ lattice and those on $2 * 3 * 3$ lattice.

states subspace. At "exceptional points", the topological degenerate ground states merge and the topological degeneracy turns into non-Hermitian degeneracy. Therefore, based on a non-Hermitian toric-code model, we surprisingly find that the degeneracy of ground states can be reduced by a local Non-Hermitian perturbation. In addition, the $\mathcal{PT}$- symmetry breaking transition can be observed by fidelity susceptibility. In the end, the influence of non-Hermitian on topological order are discussed.

[1] M. S. Rudner and L. S. Levitov, Phys. Rev. Lett. **102**, 065703 (2009).
[2] K. Esaki, M. Sato, K. Hasebe, and M. Kohmoto, Phys. Rev. B **84**, 205128 (2011).
[3] Y. C. Hu and T. L. Hughes, Phys. Rev. B **84**, 153101 (2011).
[4] S.-D. Liang and G.-Y. Huang, Phys. Rev. A **87**, 012118 (2013).
[5] B. Zhu, R. Lü, and S. Chen, Phys. Rev. A **89**, 062102 (2014).
[6] T. E. Lee, Phys. Rev. Lett. **116**, 133903 (2016).
[7] P. San-Jose, J. Cayao, E. Prada, and R. Aguado, Sci. Rep. **6**, 21427 (2016).
[8] D. Leykam, K. Y. Bliokh, C. Huang, Y. D. Chong, and F. Nori, Phys. Rev. Lett. **118**, 040401 (2017).
[9] H. Shen, B. Zhen, and L. Fu, Phys. Rev. Lett. **120**, 146402 (2018).
[10] S. Lieu, Phys. Rev. B **97**, 045106 (2018).
[11] Y. Xiong, J. Phys. Commun. **2**, 035043 (2018).
[12] K. Kawabata, Y. Ashida, H. Katsura, and M. Ueda, Phys. Rev. B **98**, 085116 (2018).
[13] Z. Gong, Y. Ashida, K. Kawabata, K. Takasan, S. Higashikawa, and M. Ueda, Phys. Rev. X **8**, 031079 (2018).
[14] S. Yao, and Z. Wang, Phys. Rev. Lett. **121**, 086803 (2018).
[15] S. Yao, F. Song, and Z. Wang, Phys. Rev. Lett. **121**, 136802 (2018).
[16] F. K. Kunst, E. Edvardsson, J. C. Budich, and E. J. Bergholtz, Phys. Rev. Lett. **121**, 026808 (2018).
[17] C. Yin, H. Jiang, L. Li, R. Lü, and S. Chen, Phys. Rev. A **97**, 052115 (2018).
[18] K. Kawabata, K. Shiozaki, and M. Ueda, Phys. Rev. B **98**, 165148 (2018).
[19] V. M. M. Alvarez, J. E. B. Vargas, M. Berdakin, and L. E. F. F. Torres, Eur. Phys. J. Spec. Top. **227**, 1295 (2018).
[20] H. Jiang, C. Yang, and S. Chen, Phys. Rev. A **98**, 052116 (2018).
[21] A. Ghatak and T. Das, J. Phys.: Condens. Matter **31**, 263001 (2019).
[22] J. Avila, F. Peñranda, E. Prada, P. San-Jose, and R. Aguado, Commun. Phys. **2**, 1 (2019).
[23] L. Jin and Z. Song, Phys. Rev. B 99, 081103 (2019);S. Lin, L. Jin, and Z. Song, Phys. Rev. B 99, 165148 (2019); K. L. Zhang, H. C. Wu, L. Jin, and Z. Song, Phys. Rev. B 100, 045141 (2019).
[24] C. H. Lee and R. Thomale, Phys. Rev. B **99**, 201103(R) (2019).
[25] T. Liu, Y.-R. Zhang, Q. Ai, Z. Gong, K. Kawabata, M. Ueda, and F. Nori, Phys. Rev. Lett. **122**, 076801 (2019).
[26] K. Kawabata, K. Shiozaki, M. Ueda, and M. Sato, Phys. Rev. X **9**, 041015 (2019).
[27] H. Zhou and J. Y. Lee, Phys. Rev. B **99**, 235112 (2019).
[28] C. H. Liu, H. Jiang, S. Chen, Phys. Rev. B **99**, 125103 (2019).
[29] E. Edvardsson, F. K. Kunst, and E. J. Bergholtz, Phys. Rev. B **99**, 081302(R) (2019).
[30] L. Herviou, J. H. Bardarson, and N. Regnault, Phys. Rev. A **99,** 052118 (2019).
[31] K. Yokomizo and S. Murakami, Phys. Rev. Lett. 123, 066404 (2019).
[32] F. K. Kunst and V. Dwivedi, Phys. Rev. B **99**, 245116 (2019).
[33] R. Chen, C.-Z. Chen, B. Zhou, and D.-H. Xu, Phys. Rev. B **99**, 155431 (2019).
[34] T. S. Deng and W. Yi, Phys. Rev. B **100**, 035102 (2019).
[35] F. Song, S. Yao, and Z. Wang, Phys. Rev. L **123**, 170401 (2019).
[36] X. W. Luo and C. Zhang, Phys. Rev. Lett. **123** 073601 (2019).
[37] S. Longhi, Phys. Rev. Research **1**, 023013 (2019).
[38] H Jiang, R Lü, S Chen, arXiv:1906.04700.
[39] Cui-Xian Guo, Xiao-Ran Wang, Su-Peng Kou, arXiv:1907.06699.
[40] N. Matsumoto, K. Kawabata, Y. Ashida, S. Furukawa, and M. Ueda, arXiv:1912.09045.
[41] Bei Zeng, and Xiao-Gang Wen, arXiv:1406.5090.
[42] S. Trebst, P. Werner, M. Troyer, K. Shtengel, and C. Nayak, Phys. Rev. Lett. **98**, 070602 (2007).
[43] X.-G. Wen, *Quantum Field Theory of Many-Body Systems*, (Oxford Univ. Press, Oxford, 2004).
[44] A. Kitaev, Annals Phys. **303**, 2 (2003). A. Kitaev, Annals

Phys. **321**, 2 (2006).
[45] X. G. Wen, Phys. Rev. Lett. **90**, 016803 (2003). X. G. Wen, Phys. Rev. **D 68**, 065003 (2003).
[46] S. P. Kou, Phys. Rev. Lett. **102**, 120402 (2009). J. Yu and S. P. Kou, Phys. Rev. B **80**, 075107 (2009). S. P. Kou, Phys. Rev. A **80**, 052317 (2009).
[47] H. Ramezani, et al., Phys. Rev. A **82**, 043803 (2010).
[48] C. Hang, G. Huang, and V. V. Konotop, Phys. Rev. Lett. **110**, 083604 (2013).
[49] T. E. Lee and C.-K. Chan, Phys. Rev. X **4**, 041001 (2014).
[50] J. Li, et. al., Nat. Commun. **10**, 855 (2019).
[51] H. N. Dai, et. al., Nat. Phys. **13**, 1195 (2017).